NASA TECHNICAL MEMORANDUM

NASA TM X-2169

NASA TM X-2169

PRELIMINARY INVESTIGATION OF PERFORMANCE OF A WEDGE NOZZLE APPLICABLE TO A SUPERSONIC-CRUISE AIRCRAFT

by Albert L. Johns and Robert J. Jeracki

Lewis Research Center
Cleveland, Ohio 44135

NATIONAL AERONAUTICS AND SPACE ADMINISTRATION • WASHINGTON, D. C. • FEBRUARY 1971

1. Report No.	2. Government Accession No.	3. Recipient's Catalog No.
NASA TM X-2169		

4. Title and Subtitle	5. Report Date
PRELIMINARY INVESTIGATION OF PERFORMANCE OF A WEDGE NOZZLE APPLICABLE TO A SUPERSONIC-CRUISE AIRCRAFT	February 1971
	6. Performing Organization Code

7. Author(s)	8. Performing Organization Report No.
Albert L. Johns and Robert J. Jeracki	E-5894
	10. Work Unit No. 720-03

9. Performing Organization Name and Address	11. Contract or Grant No.
Lewis Research Center National Aeronautics and Space Administration Cleveland, Ohio 44135	
	13. Type of Report and Period Covered
12. Sponsoring Agency Name and Address	Technical Memorandum
National Aeronautics and Space Administration Washington, D. C. 20546	14. Sponsoring Agency Code

15. Supplementary Notes

16. Abstract

An experimental cold-flow investigation was conducted to determine the performance of a wedge nozzle with a design pressure of 31.5. A translating outer cylindrical shroud was used to control internal expansion ratio. External flow effects were measured from takeoff to Mach 1.0 for a retracted shroud configuration. Subsonic-cruise performance was about 1 percent higher than that obtained for a conical plug nozzle. At most Mach numbers tested the nozzle efficiency was rather insensitive to nozzle pressure ratio. This insensitivity to pressure ratio probably resulted from low external drag. In addition, the projected area of the primary flap was only 4.8 percent of the maximum model area. Nozzle efficiency at supersonic cruise was about 1 percent lower than that obtained with a typical axisymmetric ejector nozzle.

17. Key Words (Suggested by Author(s))	18. Distribution Statement
Propulsion Nozzle	Unclassified - unlimited

19. Security Classif. (of this report)	20. Security Classif. (of this page)	21. No. of Pages	22. Price*
Unclassified	Unclassified	34	$3.00

*For sale by the National Technical Information Service, Springfield, Virginia 22151

PRELIMINARY INVESTIGATION OF PERFORMANCE OF A WEDGE NOZZLE APPLICABLE TO A SUPERSONIC-CRUISE AIRCRAFT

by Albert L. Johns and Robert J. Jeracki

Lewis Research Center

SUMMARY

An experimental cold-flow investigation was conducted in the Lewis Research Center's static test facility and 8- by 6-Foot Supersonic Wind Tunnel to determine the performance characteristics of a wedge nozzle applicable to a supersonic-cruise aircraft. This nozzle was designed for an afterburning turbojet engine and had a design nozzle pressure ratio of 31.5. Three external shroud lengths were tested in the static test facility to simulate translation: a retracted shroud for takeoff; an extended shroud (with and without sideplates) for supersonic cruise; and a mid-position shroud (with sideplates) for transonic acceleration. A retracted shroud configuration was also tested in the wind tunnel at subsonic speeds to determine external flow effects.

The nozzle efficiency at a supersonic-cruise pressure ratio of 29 and a corrected-secondary-weight-flow ratio of 0.025 was 97.4 percent, which was about 1 percent lower than that obtained with a typical axisymmetric ejector nozzle. Static-pressure measurements at station 8 plane (slightly downstream of the geometric throat) indicated a somewhat distorted velocity distribution. The flow was sonic over most of the wedge surface near the throat but was slightly supersonic ($M = 1.2$) in the corners and along the inner surface of the primary flap. As a result of the throat flow distortion, the pressures along the sides of the wedge were initially lower than those on the wedge centerline immediately downstream of the throat station.

The nozzle efficiency and pumping characteristics at takeoff were sensitive to the external shroud position. The pumping characteristics were improved by extending the shroud but the efficiency was reduced from 96.5 to 94 percent. The efficiency of the wedge nozzle was about 1 percent lower than that of a conical plug configuration during dry acceleration but was 1 percent higher than the conical plug at subsonic cruise. The wedge nozzle provided a thrust efficiency of about 93 percent at Mach 0.9 over a range of nozzle pressure ratios from 3.20 to 5.70. The insensitivity to pressure ratio probably resulted from low external drag.

INTRODUCTION

As part of a program in airbreathing propulsion, the Lewis Research Center is evaluating various exhaust nozzle concepts for application to supersonic-cruise aircraft. These nozzles must operate efficiently over a wide range of flight conditions and engine power settings. Such requirements necessitate extensive variations in nozzle geometry, including both the primary and secondary flow areas. The performance of several nozzle concepts designed for supersonic-cruise application has been studied and reported. These include a variable flap ejector (ref. 1), an auxiliary inlet ejector (ref. 2), and a low-angle conical plug nozzle (ref. 3). A fourth configuration that could be of interest is a wedge nozzle. This concept is similar to that of the plug nozzle but utilizes a two-dimensional wedge rather than a conical plug so that alternate solutions to the mechanical and cooling problems of the axisymmetric plug can be considered. The mechanics of achieving a variable-area throat may be simplified by varying a portion of the wedge surface. Accessibility for secondary cooling air is also improved through the sides of the wedge. This cooling air can be used to cool the actuator mechanism and wedge surfaces and can be discharged rearward through the trailing edge of the wedge. This flow can also be utilized for base bleed, if a truncated wedge proves to be of interest. In a manner similar to that of the plug nozzle, a cylindrical shroud is translated to regulate the internal expansion.

This report documents the performance of a low-angle wedge nozzle with a design nozzle pressure ratio of 31.5. The nozzle was only evaluated in the afterburner-off configuration with a throat to maximum internal exit-area ratio of 0.26. Static test results are presented for three different shroud positions. Effects of external flow with the retracted shroud were obtained at subsonic speeds.

SYMBOLS

A area

D drag

d diameter

F thrust

L axial length of wedge (used in static test facility) from station 8 plane to tip, 16.17 in. (41.07 cm)

l length

M Mach number

P	total pressure
$\overline{P}$	average pressure
p	static pressure
R	internal radius of primary duct (station 7)
r	radial distance from centerline
T	total temperature
w	weight-flow rate
$\left(\frac{w_s}{w_p}\right)\sqrt{\frac{T_s}{T_p}}$	corrected secondary-weight-flow-rate ratio, $\omega\sqrt{\tau}$
x	axial distance measured from station 8 plane
θ	circumferential position, deg

Subscripts:

i	ideal
j	jet
max	maximum
p	primary
s	secondary
x	condition at axial distance x from the nozzle lip
z	condition at lateral distance z from the centerline at station 8 plane
0	ambient
1, 2, 3	wind tunnel model stations (see fig. 7)
7	nozzle inlet
8	nozzle lip
9	nozzle exit

APPARATUS AND PROCEDURE

Static Test Facility

Installation. - The internal performance of the 12.06-inch (30.6-cm) wedge nozzle was obtained in the Lewis Research Center's static test stand, SW-21 (fig. 1). The

nozzle was installed in a test chamber that was connected to the laboratory combustion air and altitude exhaust facilities. The nozzle was mounted from an adapter section that contained a bellmouth inlet for the primary air supply. The adapter section was rigidly attached to a bedplate that was freely suspended by four flexure rods. Both external and internal pressure forces acting on the nozzle, bellmouth, and adapter were transmitted from the bedplate through a bell crank to a calibrated balanced-air-pressure-diaphragm load cell which was used in measuring thrust. A labyrinth seal around the inlet section ahead of the adapter sealed the primary inlet air from the exhaust plenum chamber. The space between the two labyrinth seals was vented to the test chamber to decrease the pressure differential across the second labyrinth seal. This prevented a pressure gradient on the outside of the diffuser section and minimized the flow of air under the labyrinth seal. Total-pressure and wall-static-pressure measurements were used at the bellmouth inlet to compute inlet momentum.

The nozzle primary airflow w_p was calculated from pressure and temperature measurements at the air metering station (fig. 1) and an effective area was determined by an ASME calibration nozzle. The secondary airflow w_s was measured by means of a standard ASME flowmetering orifice in the external supply line.

Nozzle pressure ratio was set by maintaining a constant nozzle inlet pressure P_7 and varying the tank pressure p_0 with the use of exhausters. Each configuration was tested over a range of pressure ratios appropriate for each shroud position.

Thrust measurement. - Jet thrust was calculated from load-cell measurements corrected for tare forces. The measured mass-flow rates were used to calculate ideal jet thrusts for each flow, assuming isentropic expansion from their measured total pressures (P_7, P_s) to p_0. The data are presented in the form of nozzle gross thrust coefficient:

$$\text{Nozzle gross thrust coefficient} = \frac{F_j}{F_{i,p}}$$

A nozzle efficiency parameter is also presented and defined as the ratio of jet thrust to the combined ideal thrust of the primary and secondary flows:

$$\text{Nozzle efficiency} = \frac{F_j}{F_{i,p} + F_{i,s}}$$

Provision was made to equate the ideal thrust of the secondary to zero if its total pressure was less than p_0. Review of the data following the test program indicated that this did occur for some of the results presented in this report. These data are identified as tailed symbols on the figures. The thrust system was calibrated by using standard ASME sonic nozzles with two different throat sizes (fig. 2). The nozzle tested herein

had a throat area of 26.21 square inches (169 sq cm) which falls between the two ASME nozzles shown. The measured performance of the ASME nozzles was compared with theoretical performance calculated from ASME flow and velocity coefficients of 0.9935 and 0.996, respectively, taken from reference 4. The results indicate approximately a ±1- and ±1/2-percent scatter in force measurements with the small and large throat areas, respectively.

Nozzle configurations. - The nozzle configuration consisted of a 10° half-angle wedge centerbody attached to a simulated circular afterburner (fig. 3(a)). A secondary flow passage is provided between the primary and the outer cylindrical nacelle for cooling the simulated afterburner and primary nozzle. The ratio of minimum secondary flow area to maximum exit area was arbitrarily selected to be 0.083. Cutouts in the sides of the wedge provided access for secondary flow for plug cooling air or for base bleed with truncated wedge configurations. The nozzle throat area was fixed in the supersonic-cruise configuration with a throat area to maximum internal exit area ratio of 0.26, which resulted in a design pressure ratio of 31.5. The maximum primary flap angle of 10° occurred only at the plan view centerline (top and bottom) and washed out to 0° at the sides of the wedge (fig. 3(b)). A cylindrical outer shroud is translated to regulate internal expansion. The shroud is retracted at low pressure ratios and extended as pressure ratio increases. Translation was simulated in this test through the use of three fixed-length shrouds (fig. 3(c)). Henceforth, these three shroud lengths are referred to as retracted, mid-position, and extended. The extended shroud length was determined such that the initial Mach line from the shroud trailing edge would intercept the wedge tip. Tests were made with and without shroud sideplates which also were swept at this Mach angle (25° 30'). These sideplates were only tested on the extended and mid-position shrouds. Details of the contour of the forward portion of the wedge are shown in figure 3(d) and the coordinates are given in table I.

Instrumentation. - Primary and secondary total pressures were measured with pitot probes, as shown in figure 4. The primary total pressure at station 7 was calculated using pressures from the nine-probe area-weighted total-pressure rake and four static-pressure orifices located around the primary flow channel perimeter. Two thermocouples are also included at station 7 to determine the primary air temperature T_7. A typical primary total-pressure profile of the flow at station 7 is shown in figure 5. The flow is assumed to be circumferentially uniform. The secondary total pressure was measured with three two-probe rakes, as shown in figure 4(a). Secondary total temperature was determined from thermocouples located at 90° and 180°. The wedge contained three axial rows of 14 static-pressure orifices. The axial locations of these static-pressure orifices are given in the table with figure 4(a). Static-pressure orifices were also located in the station 8 plane (slightly downstream of the geometric throat), figure 4(b), on the wedge and just inside the cowl lip.

Installation. - One nozzle configuration was tested in the wind tunnel to determine the external flow effects at off-design speeds from static condition to Mach 1.0. The installation of this model in the wind tunnel is shown in figures 6 and 7. The details of the wedge nozzle geometry are presented in figure 8. This nozzle was a scaled-down version of the static test model but differed from the internal performance model in that the forward portion of the wedge, upstream of the nozzle throat, had a shorter leading edge to the nozzle throat, as shown in figure 8(c). The forward portion of the wedge was constructed from circular arcs with radii of curvature to model diameter ratios (r/d_{max}) of 0.71 and 0.059. The nozzle was evaluated on an 8.5-inch (21.6-cm) jet-exit model mounted in the transonic test section of the Lewis 8- by 6-Foot Supersonic Wind Tunnel. The grounded portion of the model (fig. 7) was supported from the tunnel ceiling by a thin vertical strut with a 50.25-inch (127.63-cm) chord and a thickness-to-chord ratio of 0.035. This straight strut had leading- and trailing-edge wedge angles of 10°. The model used a closed nose with an l/d_{max} of 3.0, followed by a cylindrical section back to the nozzle attachment station. Primary and secondary air were provided by means of airflow supply lines which entered the model through the hollow support strut (fig. 7). Both flow rates were measured by means of standard ASME sharp-edge flowmetering orifices located in the external supply lines. These flows were brought through the strut at high pressure and velocity to minimize tube diameters and thus to maintain a thin strut. Both flows entered the model at right angles to the force axis, which eliminated the need to account for any inlet momentum forces. A uniform primary flow was maintained by using choke plates and a screen upstream of the nozzle inlet station. Both the primary and secondary flows were maintained at room temperature. Since the ambient pressure is constant in the wind tunnel for a given free-stream Mach number, nozzle pressure ratio is varied by changing the internal total pressure. Maximum nozzle pressure ratio varied from 6 at Mach zero to about 10 at Mach 1.0.

Thrust measurement. - The metric portion of the model, which includes the horizontal primary and secondary air bottles and exhaust nozzle, was cantilevered by flow tubes from supply manifolds located outside of the test section. The air bottles were supported by front and rear bearings. The axial forces acting on the floating portions of the model were transmitted to the load cell located in the nose of the model. A water-cooled jacket surrounded the load cell and maintained a constant temperature of 90° F (305.5 K) to eliminate errors in the calibration caused by variations in model temperature from aerodynamic heating. A static calibration of the load cell was obtained by applying known forces to the floating section and measuring the output of the load cell.

The load-cell readings were corrected for internal tare forces using the measured

tare pressures (p_1, p_2, and p_3) shown in figure 7. The load cell measured the axial force acting on the floating section of the model. This force included internal thrust and the external drag acting downstream of station 93.65 inches (238 cm) the location of the skin break. The model was tested only at zero degrees angle of attack.

The nozzle performance presented herein excludes the friction drag on the cylindrical portion of the floating section between stations 93.65 inches (238 cm) and 122.84 inches (312 cm). The downstream end of this section was arbitrarily selected to be the nozzle attachment station. The friction drag on the model between stations 93.65 inches (238 cm) and 122.84 inches (312 cm) was calculated using the semiempirical, flat-plate, local skin-friction coefficient from reference 5. The coefficient accounts for variations in boundary-layer thickness and flow profile with Reynolds number and free-stream Mach number. Previous measurements of the boundary-layer characteristics at the aft end of this jet-exit model (ref. 6) indicated that the profile and thickness were essentially the same as that computed for a flat plate of equal length. The average ratio of measured boundary-layer momentum thickness to model diameter was about 0.020 for the jet-exit model over the range of Mach numbers tested. The strut wake appeared to affect only a localized region near the top of the model and resulted in a lower local free-stream velocity than measured on the side and bottom. Therefore, the results of reference 5 were used without corrections for three-dimensional flow or strut interference effects. The calculated friction drag was, therefore, added to the load-cell reading to obtain the overall thrust-minus-drag of the exhaust nozzle.

The measured mass-flow rates were used to calculate ideal jet thrust for each flow, assuming isentropic expansion from their measured total pressures to p_0. Nozzle gross thrust coefficient is defined as the ratio of the measured thrust-minus-drag to the ideal thrust of the primary flow:

$$\text{Nozzle gross thrust coefficient} = \frac{F - D}{F_{i,p}}$$

The data are also presented as nozzle efficiency defined as thrust-minus-drag ratio to the ideal thrust of both the primary and secondary flows:

$$\text{Nozzle efficiency} = \frac{F - D}{F_{i,p} + F_{i,s}}$$

Nozzle configuration. - As mentioned earlier, only one configuration was tested in the wind tunnel to determine external flow effects at subsonic speeds. At these flight conditions the nozzle pressure ratio is generally low and the external shroud is retracted (fig. 8(a)). The primary throat area again was equal to 26 percent of the maximum internal exit area. This throat area was used to simulate both dry acceleration

and subsonic-cruise power settings. The primary nozzle (fig. 8(b)) was scaled down from the 12.06-inch (30.6-cm) diameter static test model. The wedge (fig. 8(c)) differed from the internal performance model in that the forward portion upstream of the nozzle throat had a shorter leading edge. This contour was modified following the wind tunnel test to improve the flow profile at the geometric throat station prior to the static test program.

Instrumentation. - The nozzle instrumentation was similar to that described for the static test. The rake used to obtain the primary total pressure was different and is shown in figure 9. Primary total-pressure profile of the flow approaching the primary nozzle is presented in figure 10. The nozzle inlet total pressure P_7 was obtained by integrating the pressure across an area-weighted rake located in the primary-flow passage (station 7).

RESULTS AND DISCUSSION

The turbojet nozzle pressure ratio schedule shown in figure 11 was used as a guide for setting the nozzle pressure ratio. This schedule is typical for an afterburning turbojet engine that is applicable to a supersonic-cruise aircraft. For each configuration, data were taken over a range of nozzle pressure ratios. Internal performance obtained from the static test facility will be discussed initially. The effect of external flow on the retracted shroud configuration will then be presented at subsonic speeds from Mach 0 (static condition) to 1.0.

Internal Performance

Supersonic-cruise configurations. - Thrust and pumping characteristics for supersonic-cruise configurations are presented as a function of nozzle pressure ratio for the extended shroud with and without sideplates in figures 12(a) and (b), respectively. The effect on internal performance of variations in corrected secondary weight flow from 0 to about 15 percent of the primary flow are also included.

The maximum nozzle pressure ratio in the static test facility was limited by the nozzle weight-flow rate and the capacity of the altitude exhausters. For the size model used, the maximum pressure ratio was limited to approximately 20. The experimental results were extrapolated to higher nozzle pressure ratios. This extrapolation is valid if the stream thrust parameter is constant and independent of the nozzle pressure ratio; that is, if the nozzle is flowing full. The extrapolation simply corrects the nozzle exit momentum for variations in $p_0 A_9$ as the free-stream pressure is reduced to increase

nozzle pressure ratio. It is evident in figures 12(a) and (b) that the stream thrust parameter was constant and independent of nozzle pressure ratio at the highest pressure ratio obtained during the test. The supersonic-cruise pressure ratio for an afterburning turbojet is indicated in figure 12.

The internal performance at a supersonic-cruise pressure ratio of 29 and a corrected-secondary-weight-flow ratio of 0.025 was 97.4 percent, which was about 1 percent lower than that obtained with a typical axisymmetric ejector nozzle that was reported in reference 7. It appears that the nozzle efficiency at supersonic cruise peaked at a corrected secondary weight flow from 2.5 to 4 percent of the primary flow (fig. 12(a)). The configuration with swept sideplates (fig. 12(a)) had about 1/2 percent higher nozzle efficiency than the extended shroud without sideplates at the supersonic-cruise condition (fig. 12(b)).

Static-pressure measurements at the station 8 plane indicated a somewhat distorted velocity distribution (fig. 13). The flow was near sonic over most of the wedge surface but slightly supersonic (M = 1.24) in the corners. This was apparently caused by the intersection of the wedge and cowling tending to force the throat upstream at the edges. The measurements also indicated supersonic flow along the inner surface of the primary flap (M = 1.10 to 1.20). However, the internal statics on the flap were located very close to the base of the primary lip and could have been influenced by the low base pressure feeding in through the boundary layer.

Static-pressure measurements on the centerline of the wedge surface downstream of the throat indicated that at the design pressure ratio the flow would expand to free-stream static pressure in about 40 percent of the wedge length (fig. 14(a)) with an extended shroud. Static pressures along the sides of the wedge were initially lower than the centerline pressure but were higher over the second quarter of the wedge. The initial overexpansion of the flow along the wedge sides was consistent with the supersonic flow previously shown at the corners of the geometric throat station. The addition of sideplates increased the centerline pressure beyond $x/L = 0.70$ and increased the pressure along the sides of the wedge beyond $x/L = 0.55$.

Takeoff configurations. - The static test facility can also be used to measure performance at takeoff where external flow effects are insignificant. At this flight speed the nozzle pressure ratio is low and the external shroud would generally be retracted for peak thrust efficiency. The thrust and pumping characteristics of the retracted shroud and mid-position shroud configurations are presented in figures 15(a) and (b). The fixed primary area used in this investigation simulates a dry takeoff. For a typical takeoff pressure ratio of 3.0, the nozzle efficiency was approximately 96.5 percent with 2.5 percent corrected secondary weight flow. However, the pumping characteristics, shown in figure 16, indicate that the retracted shroud configuration will not provide secondary flow from a free-stream source. The pumping characteristics of the mid-

position shroud are somewhat improved over those of the retracted shroud at takeoff. The thrust efficiency of the mid-position shroud was about 96 percent at takeoff (fig. 15(b)), which was only a 1/2 percent lower than that obtained with the retracted shroud. It appears that the extended shroud could pump approximately 2.5 percent corrected secondary weight flow at takeoff (fig. 16). However, full extension of the shroud to improve the pumping characteristics reduced the nozzle efficiency to about 94 percent.

External Flow Effects

The configuration with the retracted shroud was tested in the wind tunnel to determine the effect of external flow on nozzle performance at subsonic speeds from Mach 0 to 1.0 (fig. 17). Thrust and pumping characteristics are presented as a function of nozzle pressure ratio for a nominal corrected-secondary-weight-flow ratio of 0.035. The fixed primary throat area simulates both dry acceleration and subsonic-cruise conditions. At most Mach numbers tested the nozzle efficiency was rather insensitive to nozzle pressure ratio. For example, at Mach 0.90 the nozzle efficiency was approximately 93 percent for a nozzle pressure ratio range from 3.2 to 5.70. The insensitivity to pressure ratio probably resulted from low external drag. The projected area of the primary flap was only 4.8 percent of the maximum model area. In addition, the primary flap angles were low, varying from a maximum of 10° at the top and bottom to 0° at the sides.

The nozzle efficiency and secondary total-pressure requirements for the wedge nozzle are compared to a conical plug nozzle at subsonic speeds for the assumed flight trajectory in figure 18. The two nozzles are compared for a dry takeoff and acceleration and also for subsonic cruise. Data are shown for nominal values of corrected-secondary-weight-flow ratio. At the dry acceleration trajectory the nozzle efficiency of the wedge was about 1 percent lower than that of the conical plug nozzle. However, at subsonic-cruise condition the wedge nozzle was about 1 percent higher in nozzle efficiency. This again probably resulted from lower external drag for the wedge nozzle compared to the conical plug. The plug nozzles from reference 8 had primary flap areas that were 18 percent of the maximum model area and flap angles from 14° to 17°. However, the wedge nozzle requires higher secondary total pressure than the conical plug nozzle during dry acceleration. The secondary total-pressure recovery of the two nozzles are similar at subsonic-cruise condition, where the secondary total pressures are about equal to free-stream static pressure p_0.

SUMMARY OF RESULTS

An experimental investigation was conducted in the Lewis Research Center's static test stand and 8- by 6-Foot Supersonic Wind Tunnel to determine the performance of a wedge nozzle with a design nozzle pressure ratio of 31.5. The nozzle throat area was fixed in the afterburner-off configuration with a throat to maximum internal exit area ratio of 0.26. Three fixed shroud positions were tested to simulate a translating outer cylindrical shroud. The corrected-secondary-weight-flow ratio was varied from 0 to 15 percent of the primary flow. Data were obtained at nozzle pressure ratios up to 20. The nozzle performance was extrapolated to the design point for the fully extended shroud configurations. An 8.5-inch (21.6-cm) wind tunnel model, scaled down from the 12.06-inch (30.6-cm) static test facility model but with a different wedge throat approach section, was tested to Mach 1.00 with a fully retracted external shroud and with a nominal corrected secondary weight flow of 3.5 percent. The following results were obtained:

1. Internal performance at a supersonic-cruise pressure ratio of 29 and a corrected secondary flow ratio of 0.025 was 97.4 percent, which was about 1 percent lower than that obtained with a typical axisymmetric ejector nozzle.

2. A configuration with swept sideplates on the translating shroud had about 1/2 percent higher nozzle efficiency performance than one without sideplates.

3. Static-pressure measurements at station 8 plane (slightly downstream of the geometric throat) indicated a somewhat distorted velocity distribution. The flow was sonic over most of the wedge surface but was slightly supersonic ($M = 1.2$) in the corners and along the inner surface of the primary flap.

4. Static-pressure measurements on the centerline of the wedge surface downstream of the throat indicated that at the design pressure ratio the flow would expand to free-stream static pressure in slightly over 40 percent of the wedge length. Static pressures toward the sides of the wedge initially were lower than the centerline pressures but were higher over the second quarter of the wedge. Addition of swept sideplates increased the centerline pressures only on the last quarter of the wedge. These sideplates were also effective in increasing pressures along the sides of the wedge over its latter half.

5. The internal performance and pumping characteristics at a takeoff pressure ratio were sensitive to the external shroud position. In general, fully extending the shroud improved the pumping characteristics but reduced the nozzle efficiency from 96.5 to 94 percent.

6. The thrust efficiency of the wedge nozzle was about 1 percent lower than that of a conical plug nozzle during dry acceleration but 1 percent higher than the conical plug at subsonic cruise.

7. From takeoff to Mach 0.90, the nozzle efficiency was rather insensitive to nozzle pressure ratio at each Mach number. For example, at Mach 0.90, a nozzle efficiency of 93 percent was obtained over a nozzle pressure ratio range from 3.20 to 5.7. This insensitivity to pressure ratio probably resulted from low external drag. The projected area of the primary flap was only 4.8 percent of the maximum model area. In addition, the primary flap angles were low, varying from a maximum of 10° at the top and bottom to 0° at the sides.

Lewis Research Center,
National Aeronautics and Space Administration,
Cleveland, Ohio, September 22, 1970,
720-03.

REFERENCES

1. Steffen, Fred W.; and Jones, John R.: Performance of a Wind Tunnel Model of an Aerodynamically Positioned Variable Flap Ejector at Mach Numbers From 0 to 2.0. NASA TM X-1639, 1968.
2. Bresnahan, Donald L.: Performance of an Aerodynamically Positioned Auxiliary Inlet Ejector Nozzle at Mach Numbers From 0 to 2.0. NASA TM X-2023, 1970.
3. Bresnahan, Donald L.: Experimental Investigation of a 10° Conical Turbojet Plug Nozzle With Iris Primary and Translating Shroud at Mach Numbers From 0 to 2.0. NASA TM X-1709, 1968.
4. Anon.: Fluid Meters, Their Theory and Application. Fifth ed., ASME, 1959.
5. Smith, K. G.: Methods and Charts for Estimating Skin Friction Drag in Wind Tunnel Test With Zero Heat Transfer. Rep. ARC-CP-824, Aeronautical Research Council, Great Britain, 1965.
6. Harrington, Douglas E.: Jet Effects on Boattail Pressure Drag of Isolated Ejector Nozzles at Mach Numbers From 0.60 to 1.47. NASA TM X-1785, 1969.
7. Shrewsbury, George D.; and Jones, John R.: Static Performance of an Auxiliary Inlet Ejector Nozzle for Supersonic-Cruise Aircraft. NASA TM X-1653, 1968.
8. Harrington, Douglas E.: Performance of an Isolated 10° Conical Plug Nozzle With Various Primary Flap and Nacelle Configurations at Mach Numbers From 0 to 1.97. NASA TM X-2086, 1970.

TABLE I. - COORDINATES OF WEDGE SURFACE

UPSTREAM OF STATION 8

Station 8

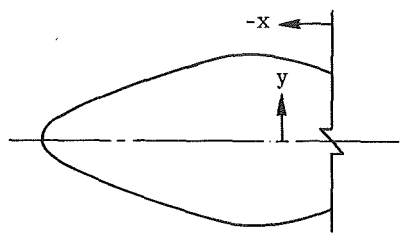

-x		±y		-x		±y	
in.	cm	in.	cm	in.	cm	in.	cm
0.000	------	2.82	7.163	4.614	11.720	1.900	4.826
.625	1.588	2.925	7.430	5.299	13.460	1.600	4.064
1.005	2.553	2.985	7.582	5.982	15.194	1.200	3.600
1.200	3.048	2.997	7.612	6.382	16.210	.900	2.286
1.535	3.899	2.975	7.556	6.584	16.723	.700	1.778
1.936	4.917	2.900	7.366	6.702	17.023	0.550	1.397
2.311	5.870	2.800	7.112	6.780	17.221	.400	1.016
2.772	7.041	2.650	6.731	6.842	17.379	.250	.635
3.175	8.064	2.500	6.350	6.863	17.432	.175	.444
3.974	10.094	2.200	5.588	6.876	17.465	.100	.254
				6.882	17.480	0	0

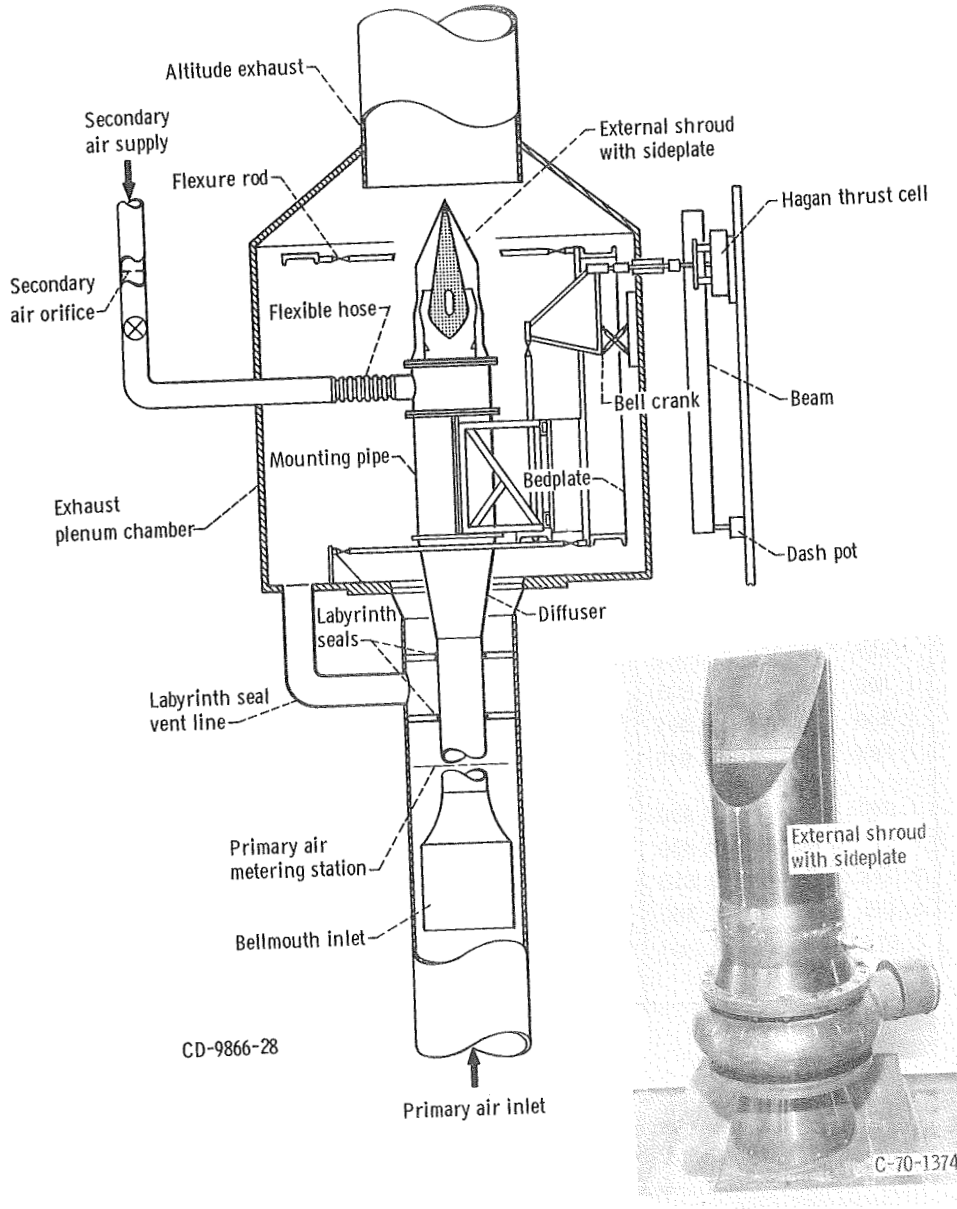

Figure 1. - Schematic view of nozzle installation in static test facility.

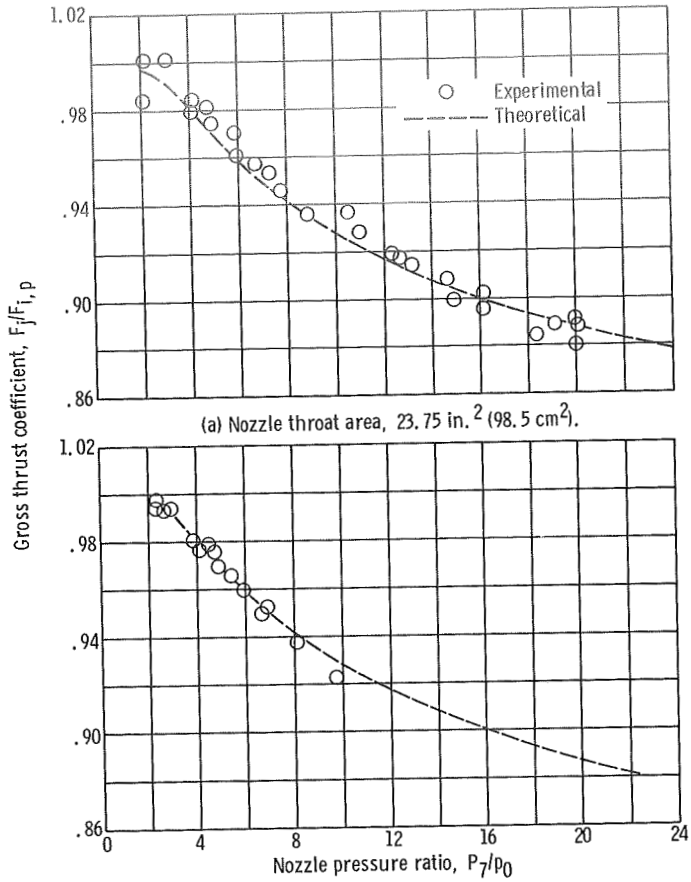

(a) Nozzle throat area, 23.75 in.^{2} (98.5 cm^2).

(b) Nozzle throat area, 55.67 in.^{2} (153.20 cm^2).

Figure 2. - Internal performance of ASME sonic nozzle in static test stand.

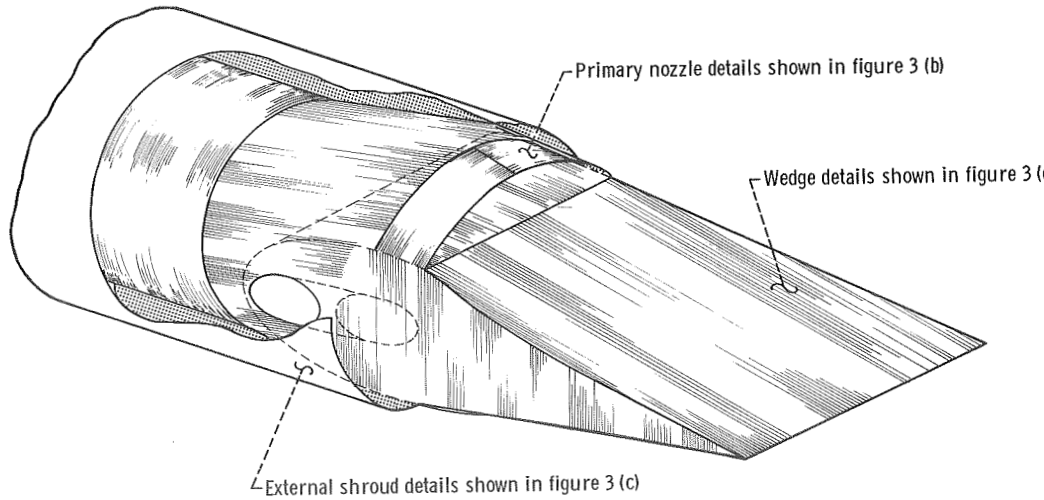

(a) Assembly of wedge nozzle.

Figure 3. - Details of static test facility wedge nozzle. (Dimensions are in inches (cm).)

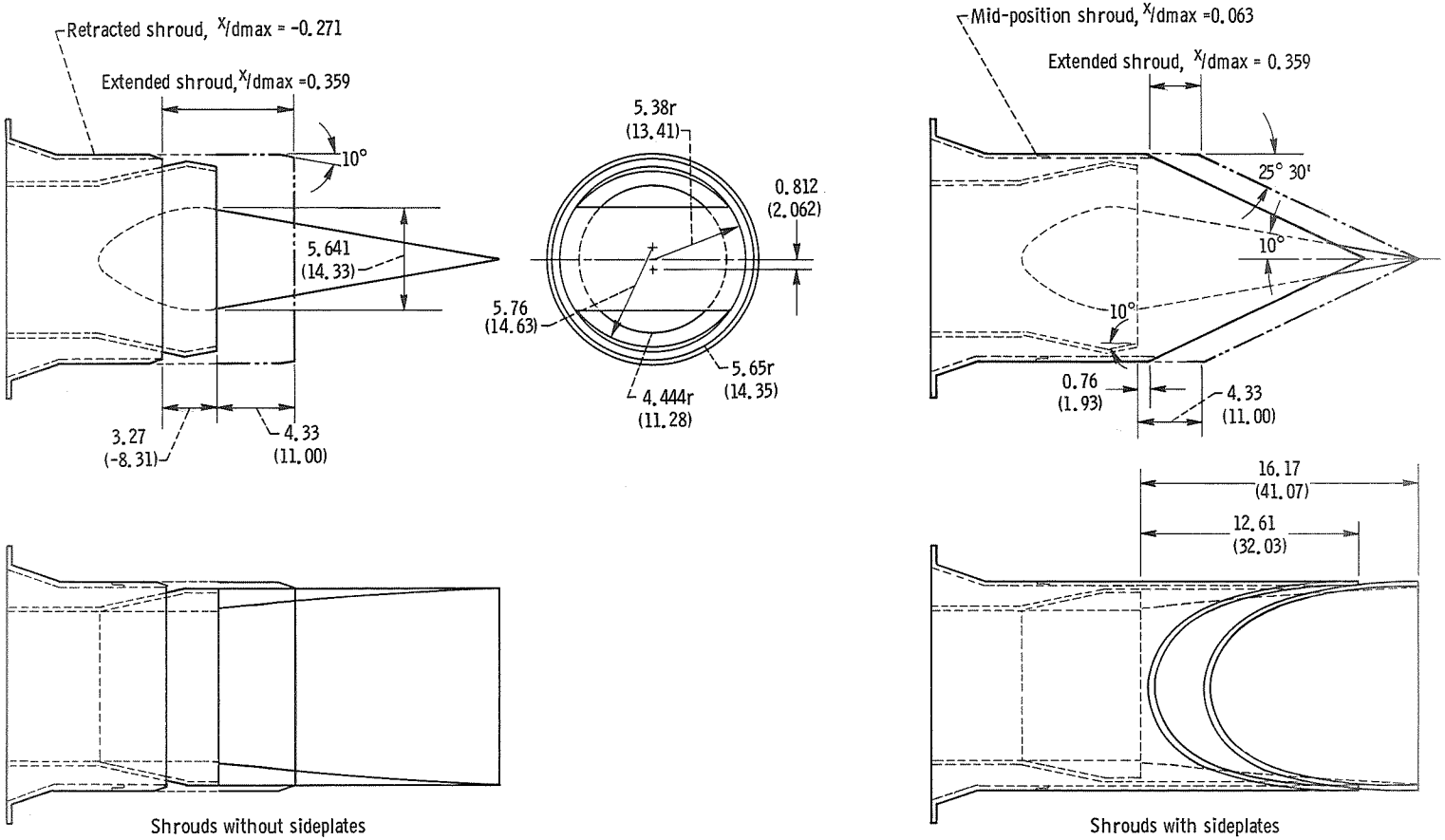

(c) External shroud dimensions and configuration definitions.

Figure 3. - Continued.

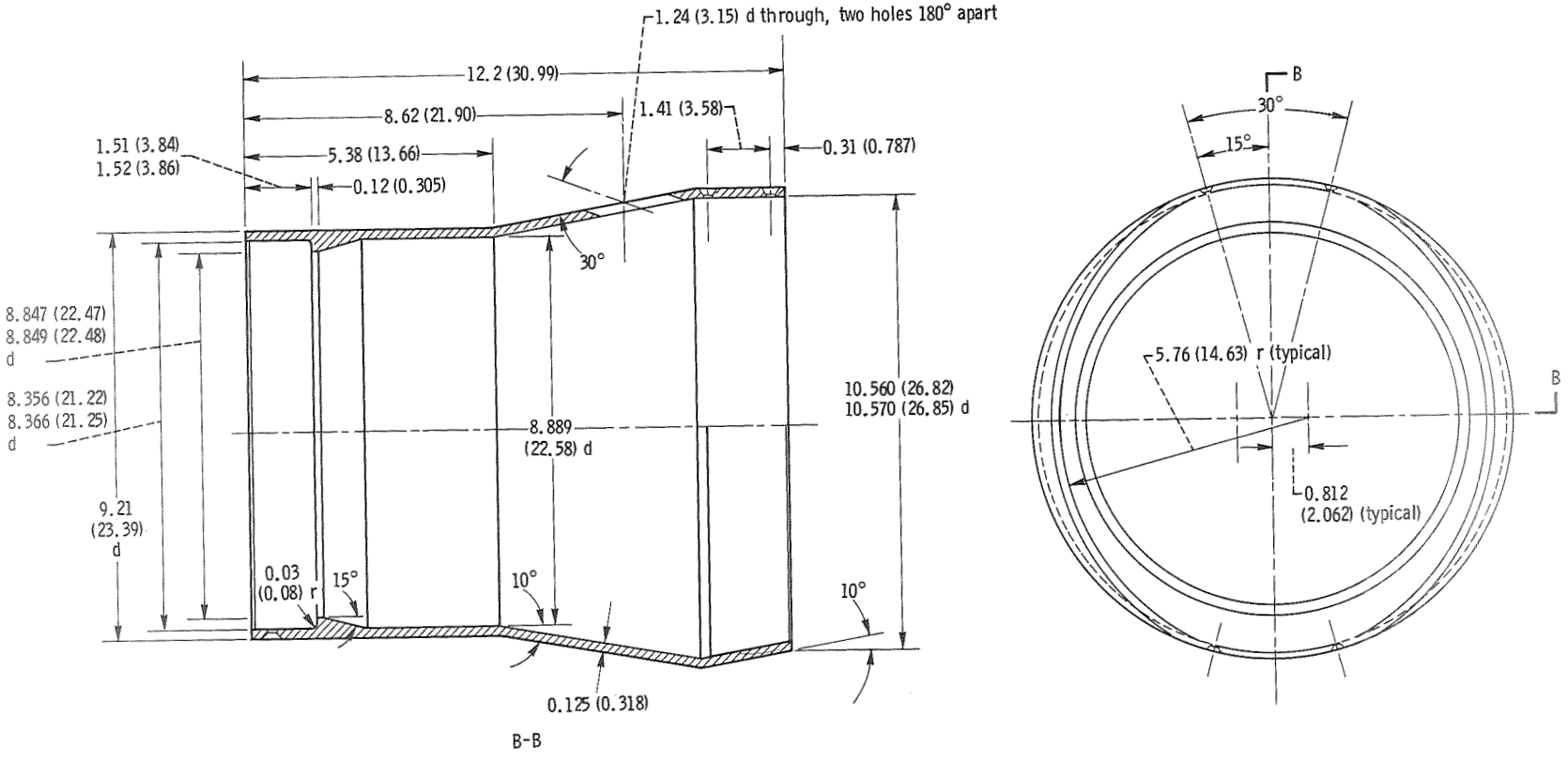

(b) Details of primary nozzle.

Figure 3. - Continued.

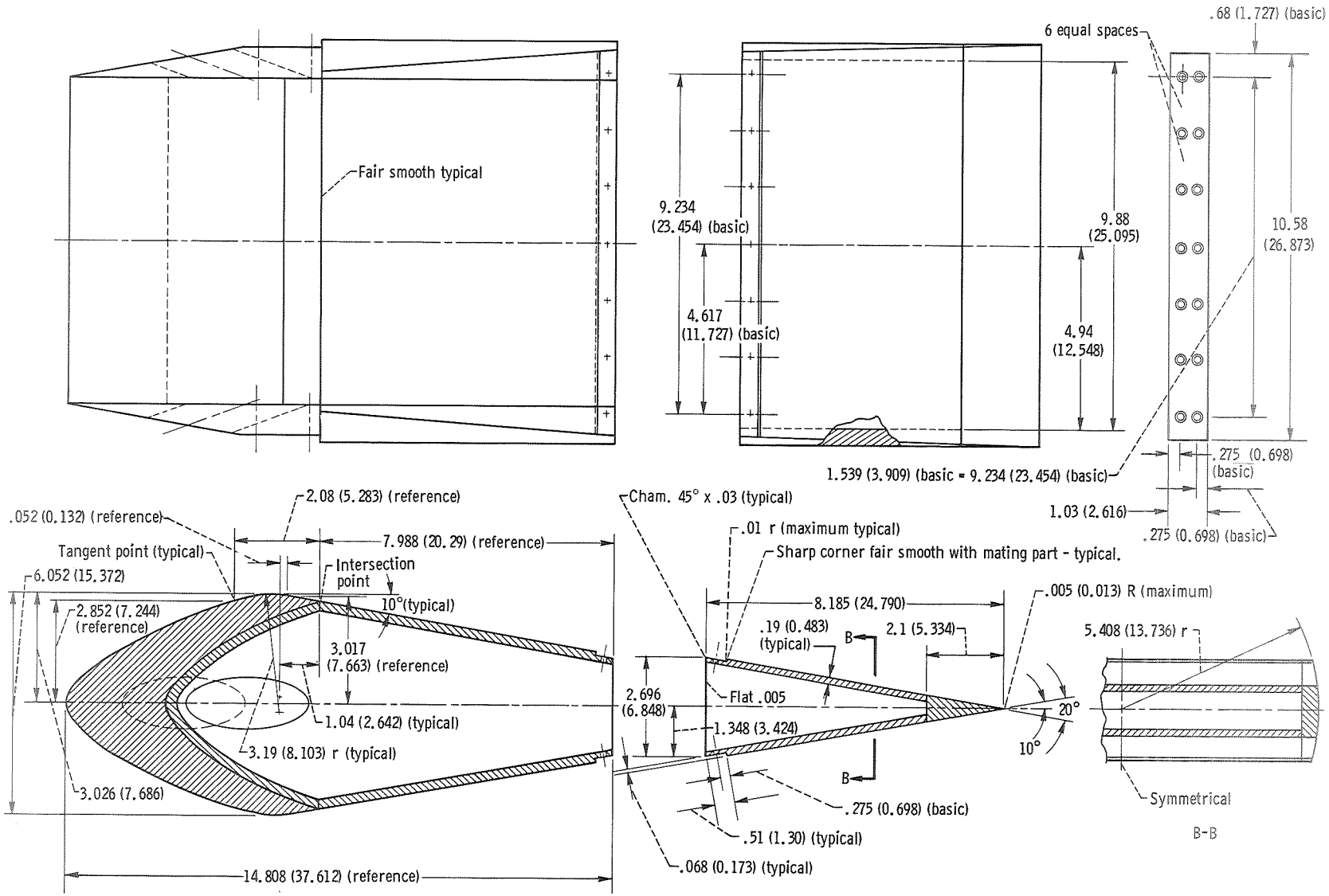

(d) Details of wedge.

Figure 3. - Concluded.

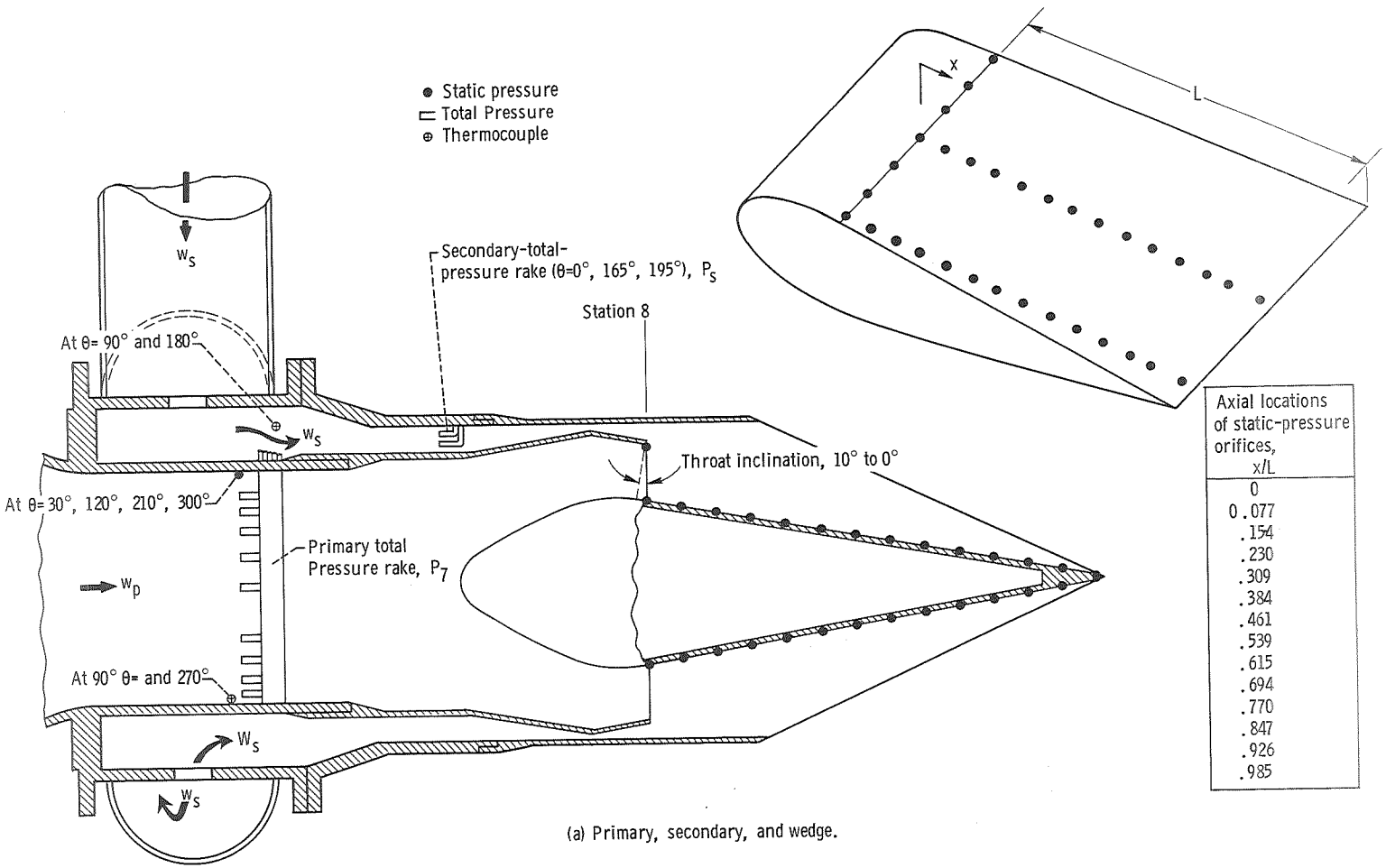

(a) Primary, secondary, and wedge.

Figure 4. - Static test facility model instrumentation.

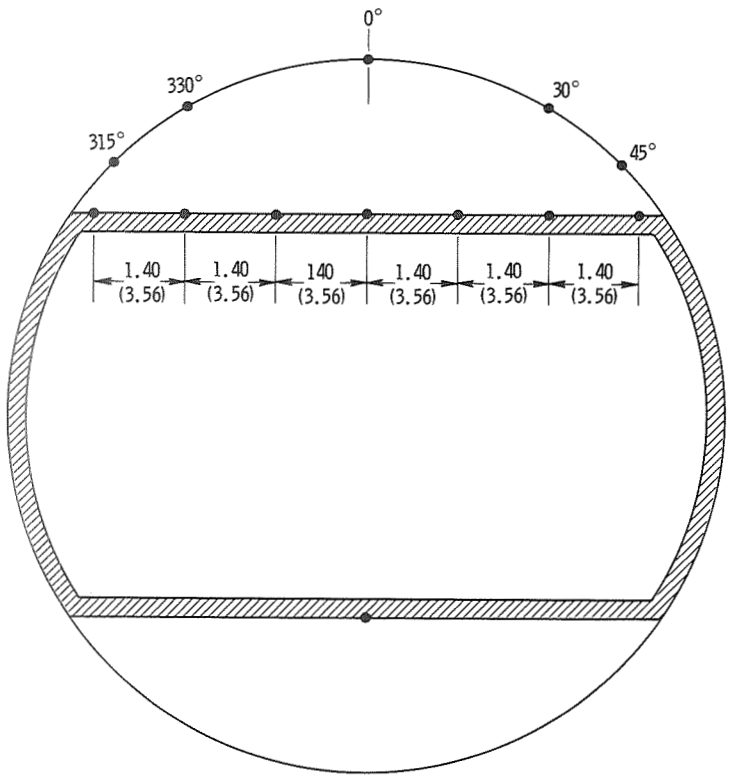

(b) Station 8. (Dimensions are in inches (cm).

Figure 4. - Concluded.

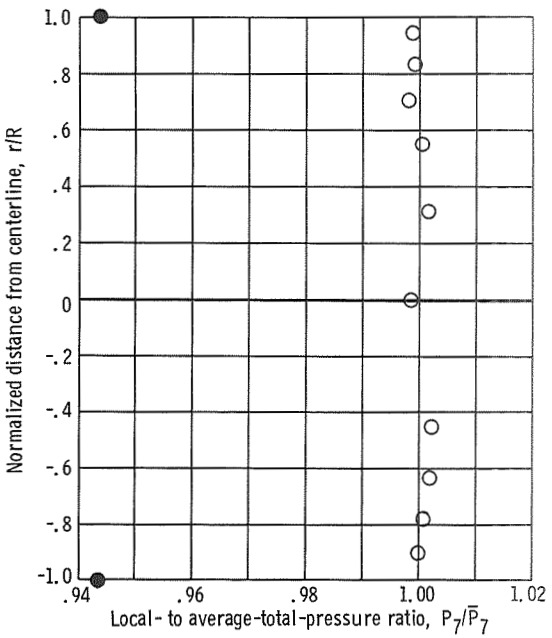

Figure 5. - Primary-total-pressure profile at station 7 in nozzle static test facility.

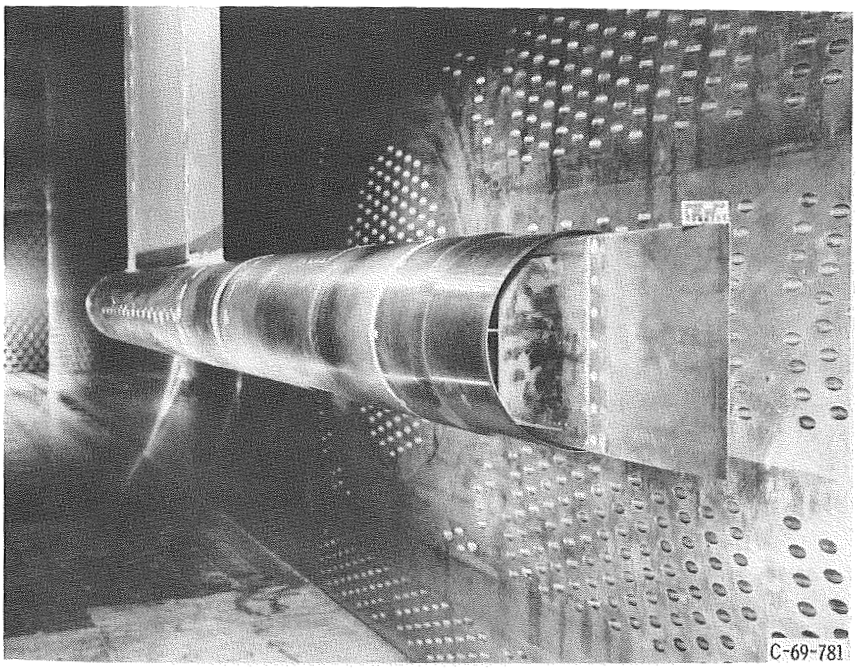

Figure 6. - 8.5-Inch (21.6-cm) wedge nozzle installed on the wind tunnel support model.

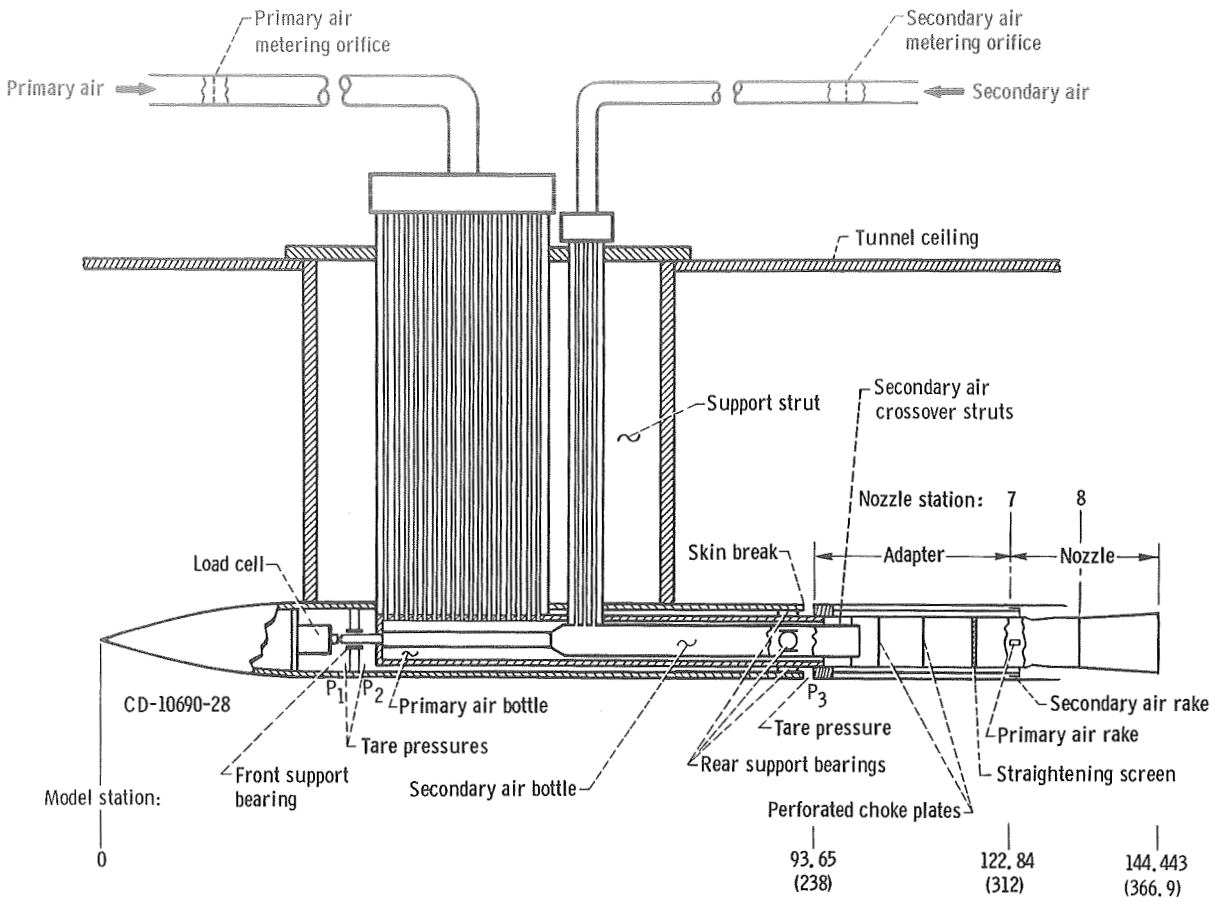

Figure 7. - Nozzle support model and thrust measuring system for 8- by 6-Foot Supersonic Wind Tunnel. (Dimensions are in inches (cm).)

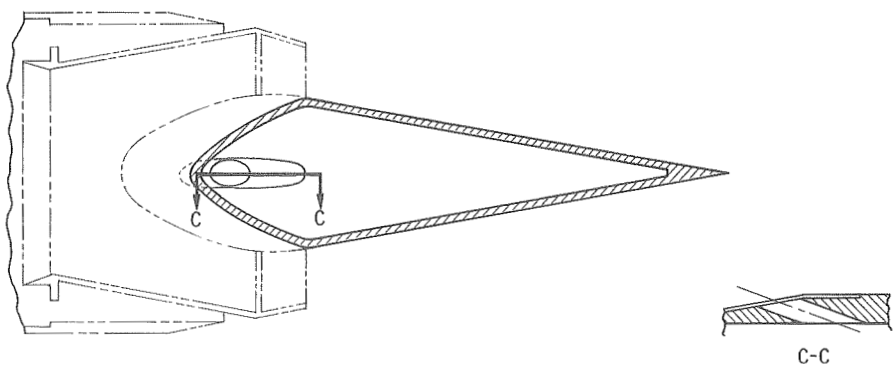

(a) Assembly of 8.5-inch (21.6-cm) wedge nozzle.

Figure 8. - Details of 8- by 6- Foot Supersonic Wind Tunnel wedge nozzle. (Dimensions are inches (cm).)

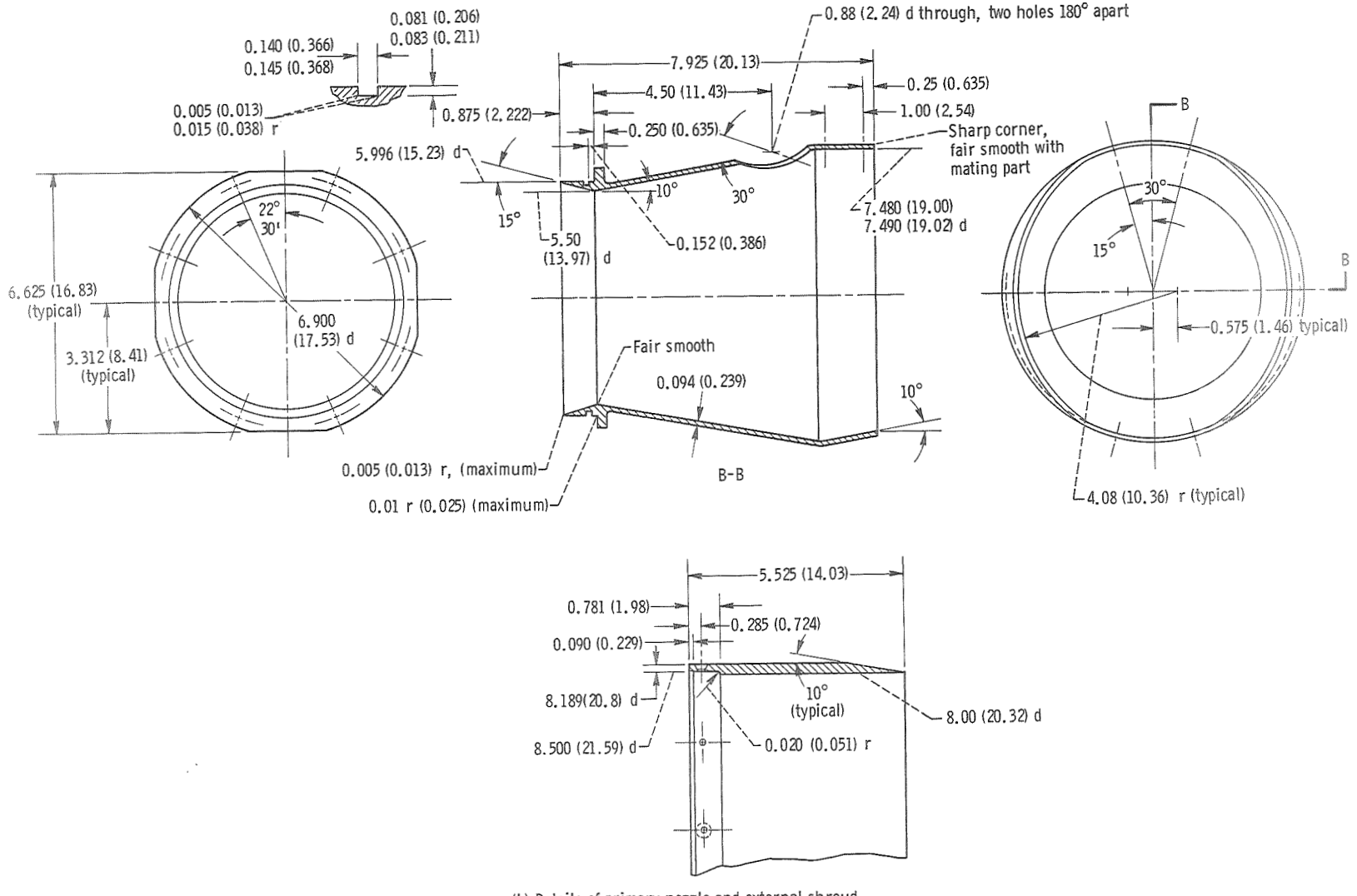

(b) Details of primary nozzle and external shroud.

Figure 8. - Continued.

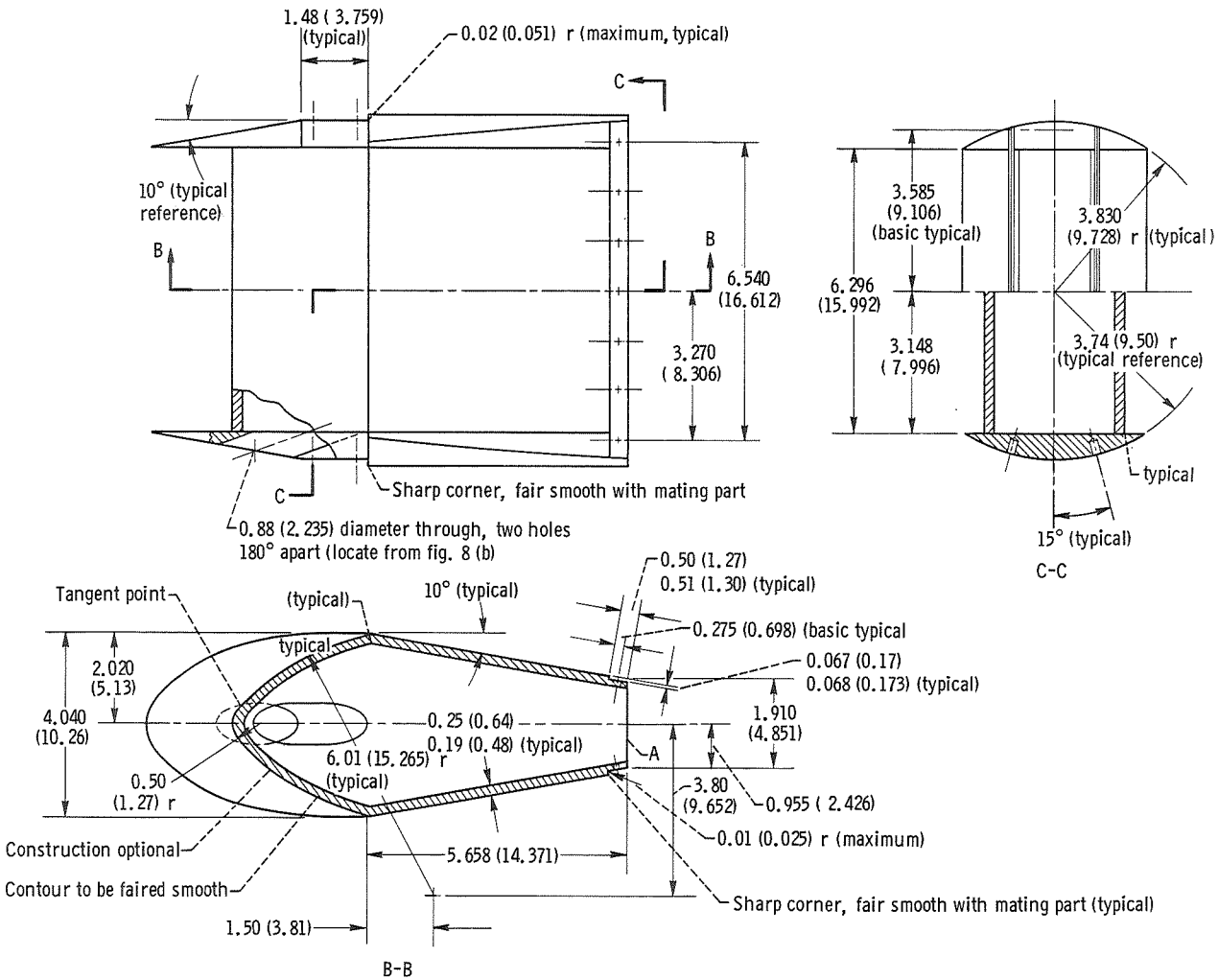

(c) Details of wedge.

Figure 8. - Concluded.

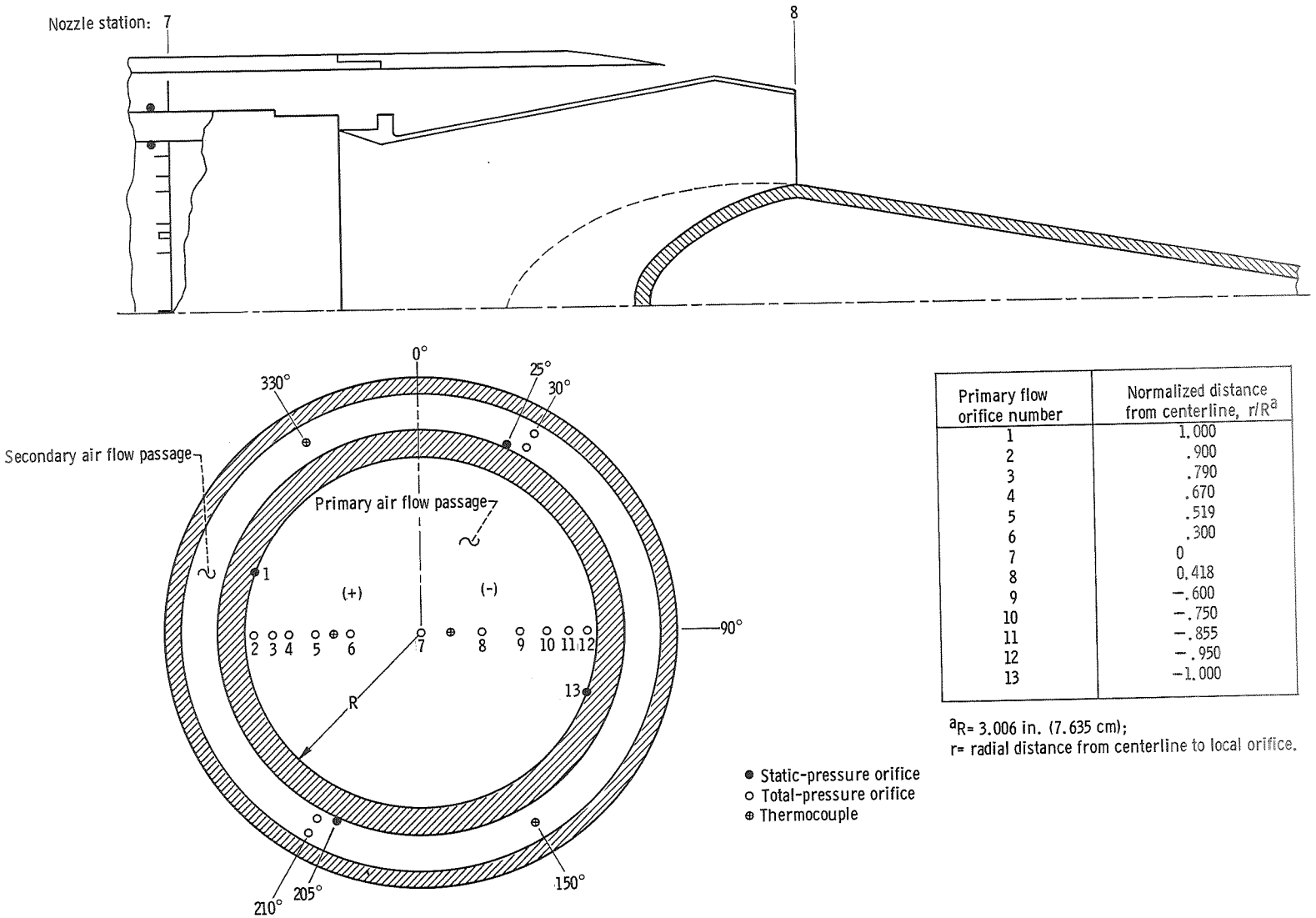

Primary flow orifice number	Normalized distance from centerline, r/R^a
1	1.000
2	.900
3	.790
4	.670
5	.519
6	.300
7	0
8	0.418
9	−.600
10	−.750
11	−.855
12	−.950
13	−1.000

[a]R= 3.006 in. (7.635 cm);
r= radial distance from centerline to local orifice.

Figure 9. - 8.5-Inch (21.6-cm) wedge nozzle instrumentation at station 7. (Dimensions are in inches (cm).)

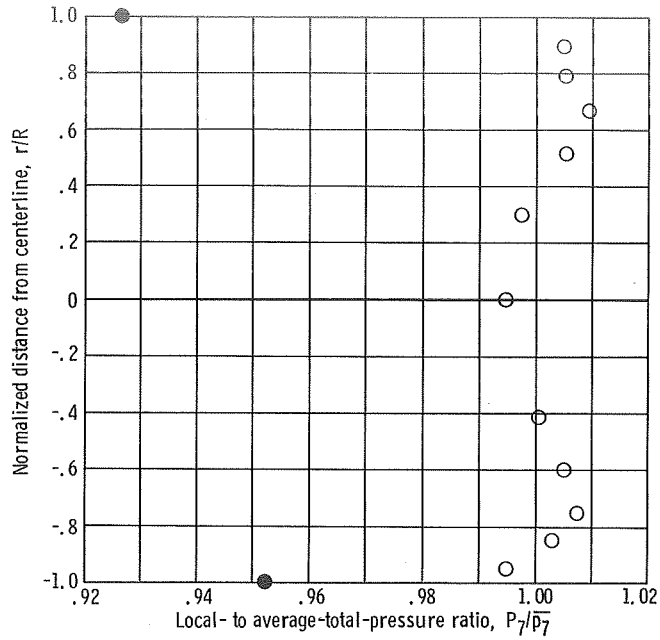

Figure 10. - Primary-total-pressure profile at station 7 in wind tunnel support model.

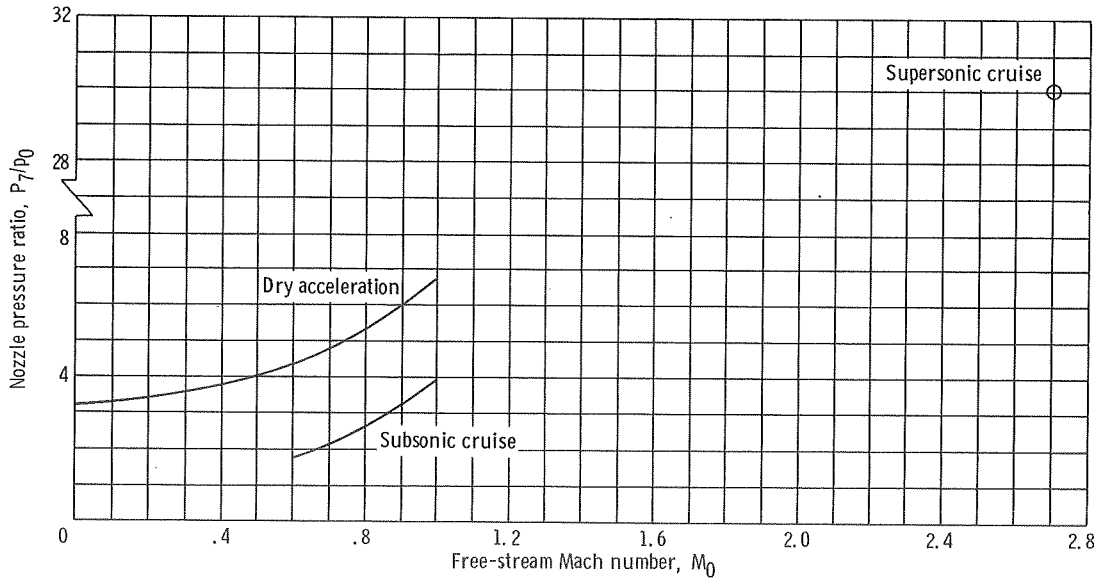

Figure 11. - Assumed nozzle pressure ratio schedule for a turbojet engine.

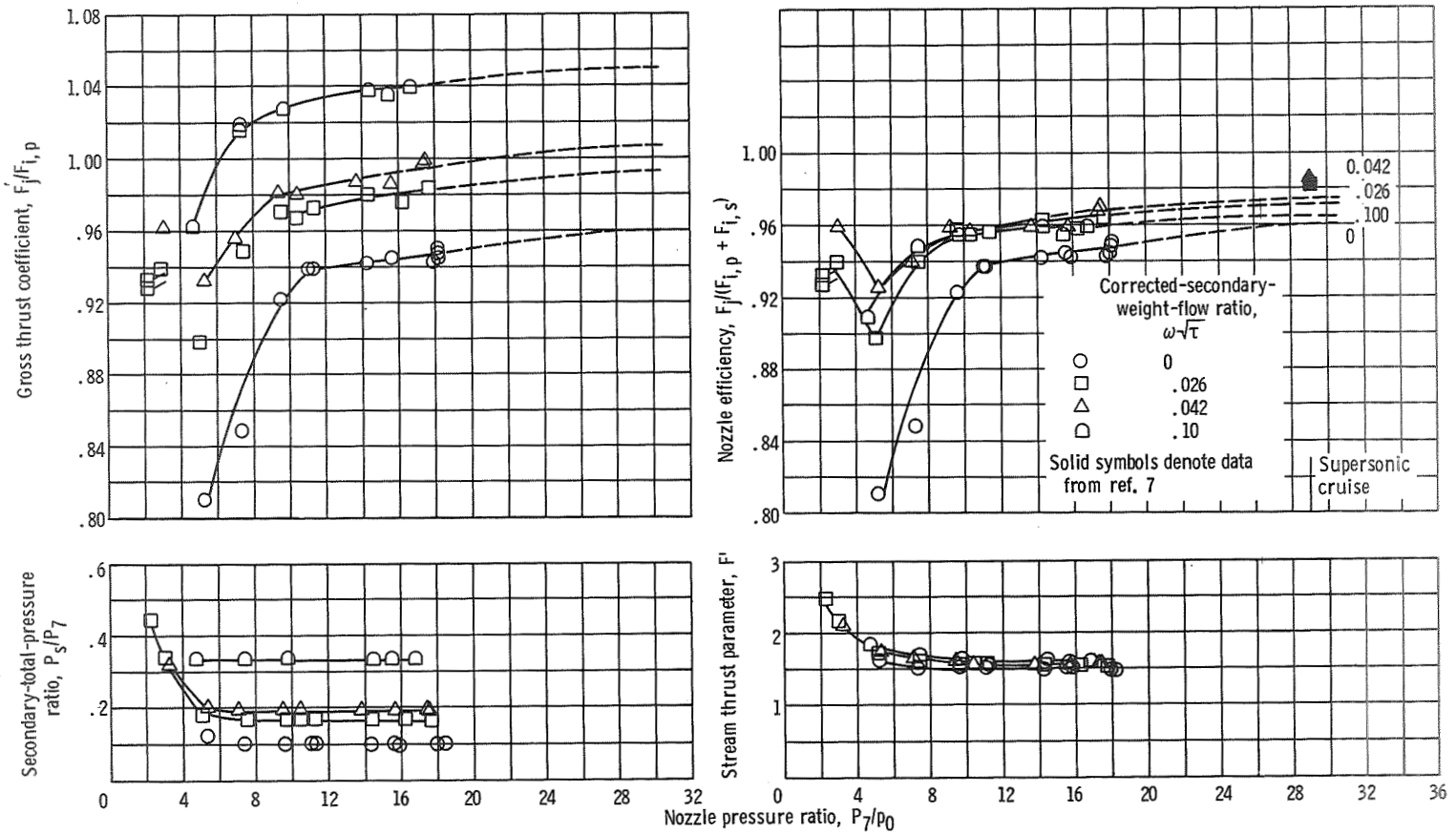

(a) Extended shroud with sideplates.

Figure 12. - Effect of nozzle pressure ratio on nozzle performance, supersonic-cruise configurations.

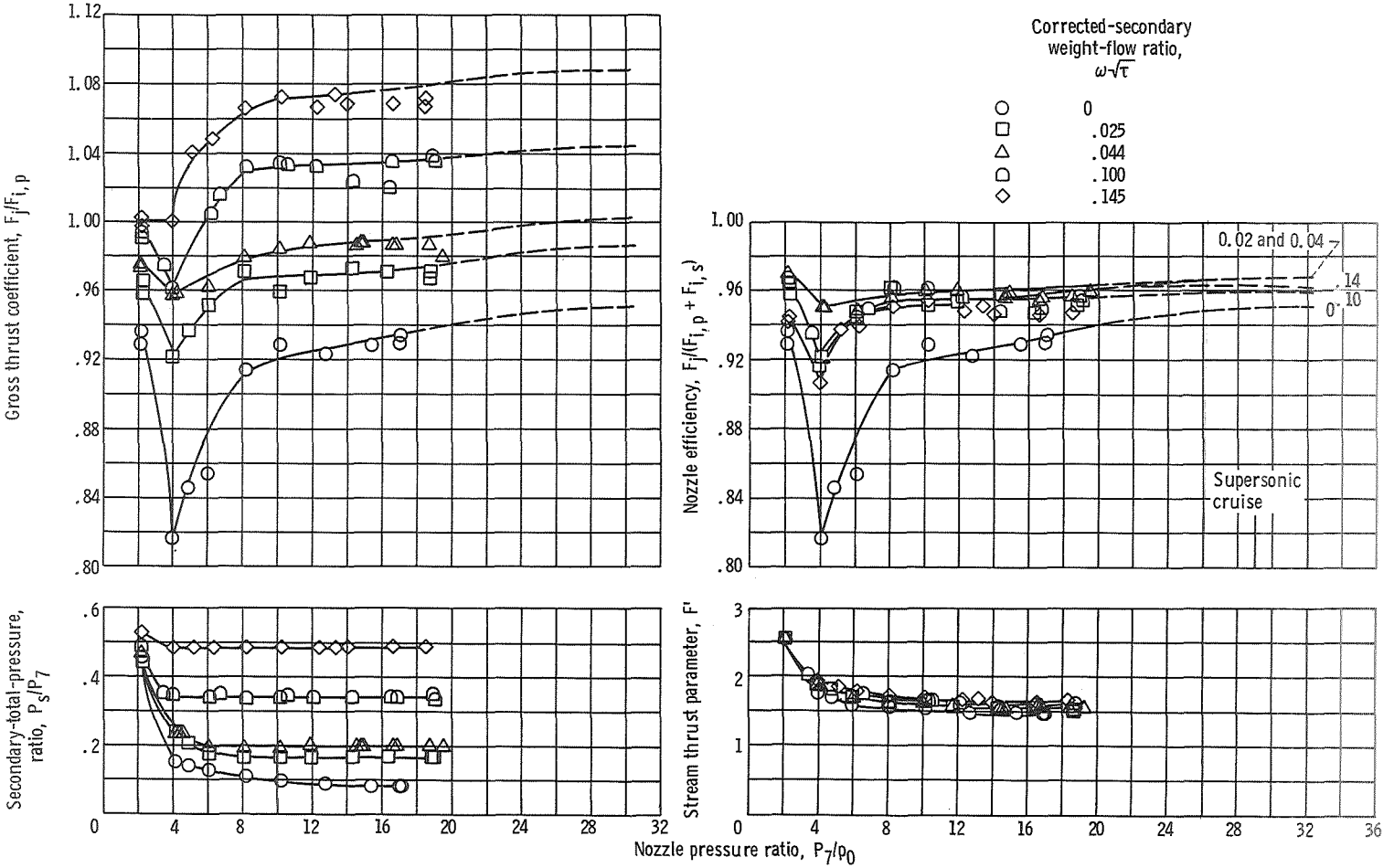

(b) Extended shroud without sideplates.

Figure 12. - Concluded.

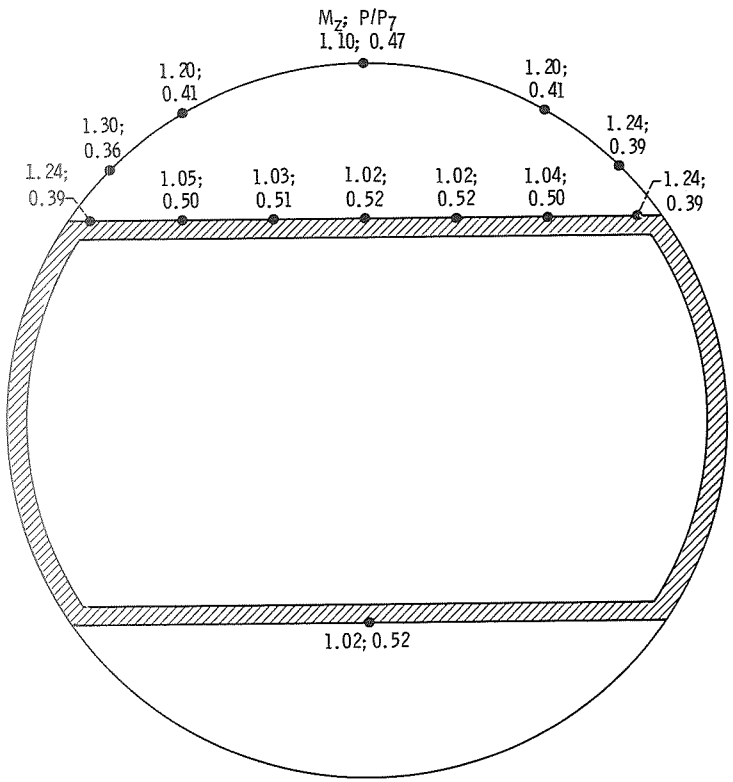

Figure 13. - Local Mach number and pressure distribution at station 8 plane; nozzle pressure ratio, P_7/P_0 = 19.

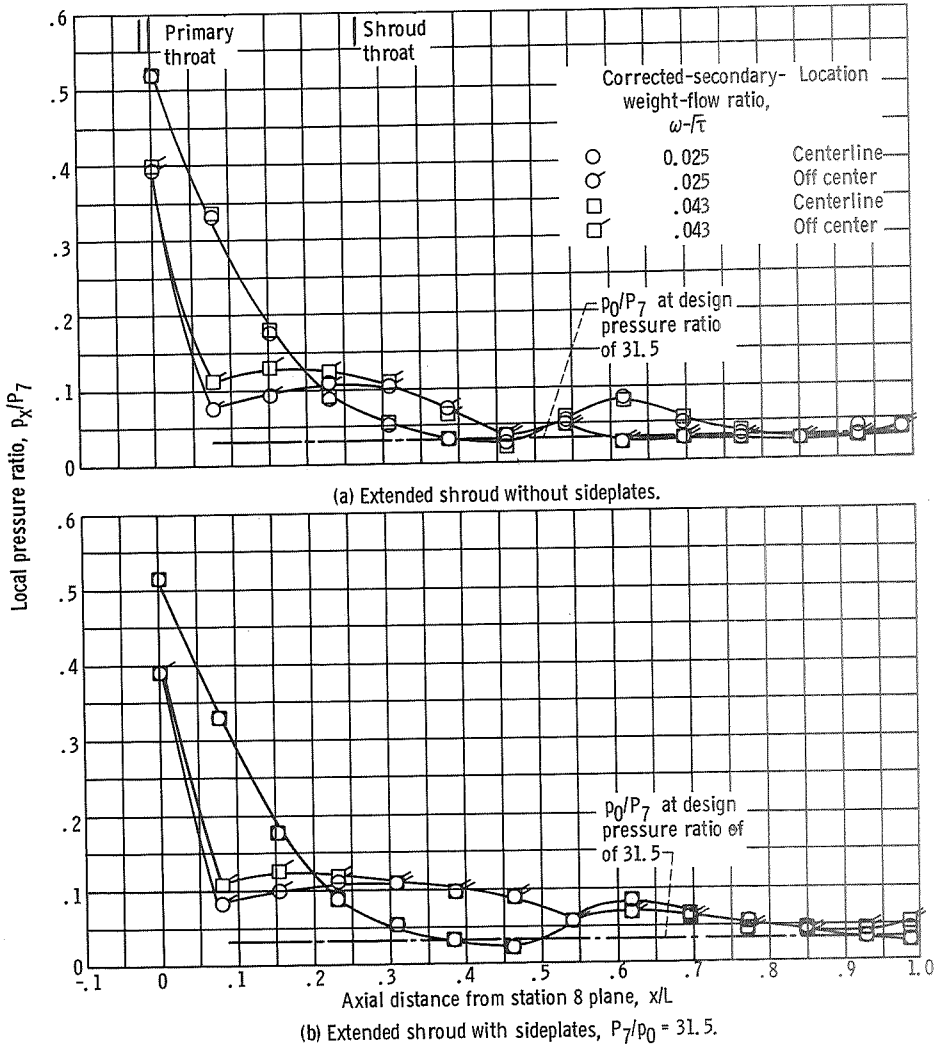

(a) Extended shroud without sideplates.

(b) Extended shroud with sideplates, P_7/p_0 = 31.5.

Figure 14. - Static-pressure distribution on wedge surface.

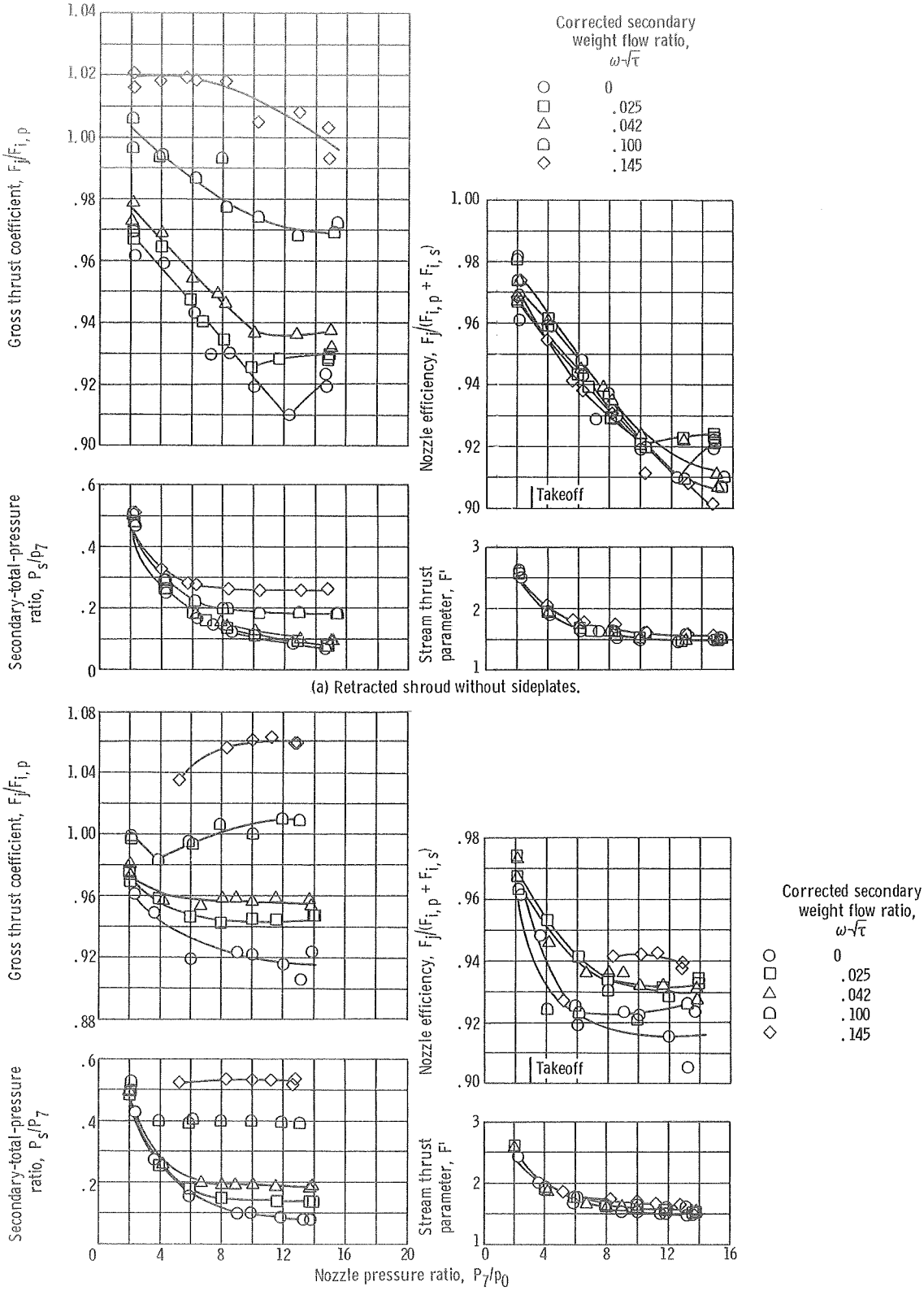

(a) Retracted shroud without sideplates.

(b) Mid-position shroud with sideplates.

Figure 15. - Effect of nozzle pressure ratio on nozzle performance, takeoff configurations.

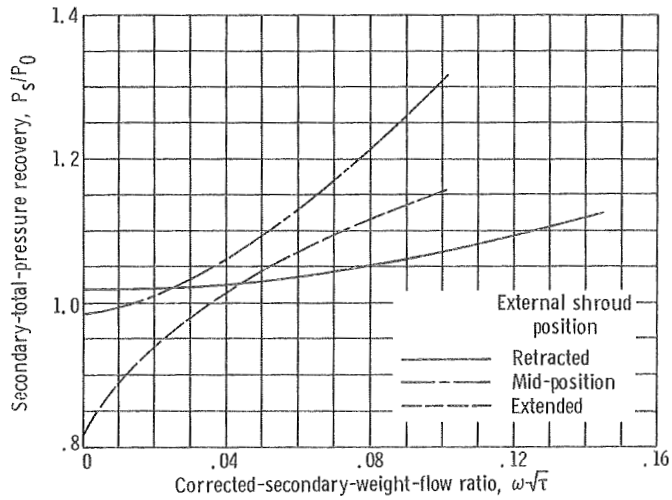

Figure 16. - Effect of external shroud position on secondary-total-pressure recovery at takeoff with a nozzle pressure ratio of 3.00.

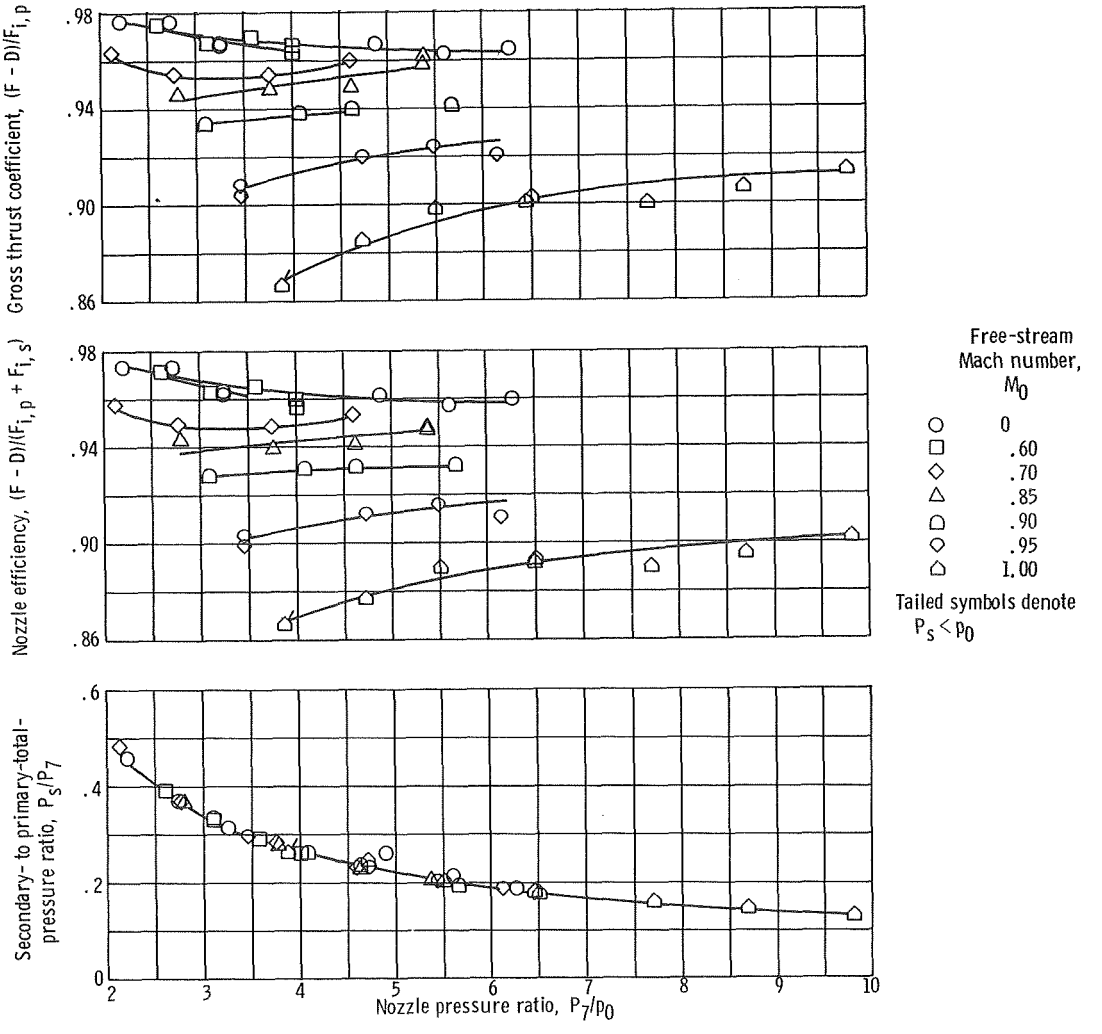

Figure 17. - External flow effects on nozzle performance characteristics with a retracted shroud for a nominal corrected-secdndary-flow-ratio, $(w_s/w_p)\sqrt{T_s/T_p} = 0.035$.

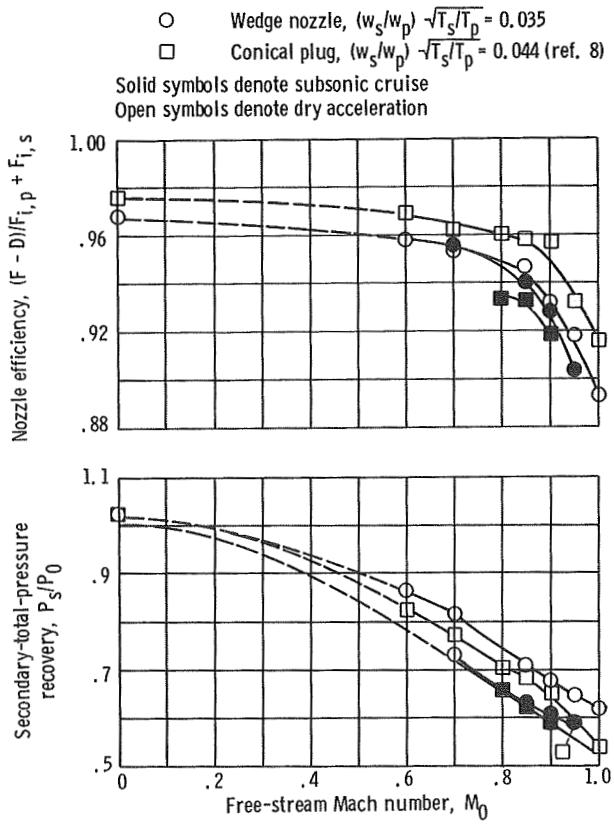

Figure 18. - Comparison of wedge nozzle to a conical plug nozzle at subsonic speeds.

NATIONAL AERONAUTICS AND SPACE ADMINISTRATION
WASHINGTON, D.C. 20546

OFFICIAL BUSINESS

FIRST CLASS MAIL

POSTAGE AND FEES PAID
NATIONAL AERONAUTICS AND
SPACE ADMINISTRATION

POSTMASTER: If Undeliverable (Section 158 Postal Manual) Do Not Return

"The aeronautical and space activities of the United States shall be conducted so as to contribute . . . to the expansion of human knowledge of phenomena in the atmosphere and space. The Administration shall provide for the widest practicable and appropriate dissemination of information concerning its activities and the results thereof."

—NATIONAL AERONAUTICS AND SPACE ACT OF 1958

NASA SCIENTIFIC AND TECHNICAL PUBLICATIONS

TECHNICAL REPORTS: Scientific and technical information considered important, complete, and a lasting contribution to existing knowledge.

TECHNICAL NOTES: Information less broad in scope but nevertheless of importance as a contribution to existing knowledge.

TECHNICAL MEMORANDUMS: Information receiving limited distribution because of preliminary data, security classification, or other reasons.

CONTRACTOR REPORTS: Scientific and technical information generated under a NASA contract or grant and considered an important contribution to existing knowledge.

TECHNICAL TRANSLATIONS: Information published in a foreign language considered to merit NASA distribution in English.

SPECIAL PUBLICATIONS: Information derived from or of value to NASA activities. Publications include conference proceedings, monographs, data compilations, handbooks, sourcebooks, and special bibliographies.

TECHNOLOGY UTILIZATION PUBLICATIONS: Information on technology used by NASA that may be of particular interest in commercial and other non-aerospace applications. Publications include Tech Briefs, Technology Utilization Reports and Technology Surveys.

Details on the availability of these publications may be obtained from:

SCIENTIFIC AND TECHNICAL INFORMATION OFFICE

NATIONAL AERONAUTICS AND SPACE ADMINISTRATION

Washington, D.C. 20546